J Mater Sci (2011) 46:875–881
DOI 10.1007/s10853-010-4828-2

Microstructural evolution of Al–Zn–Mg–Cu alloy during homogenization

**Yun-Lai Deng · Li Wan · Li-Hui Wu ·
Yun-Ya Zhang · Xin-Ming Zhang**

Received: 11 March 2010 / Accepted: 13 August 2010 / Published online: 24 August 2010

Abstract In this study, the microstructural evolution of an as-cast Al–Zn–Mg–Cu alloy (AA7085) during various homogenization schemes is investigated. It is found that in a single-stage homogenization scheme, some of the primary eutectic gets transformed into the Al_2CuMg phase at 400 °C, and the primary eutectic and Al_2Cu phase gradually dissolve into the alloy matrix at 450 °C. The Al_3Zr particles are mainly precipitated at the center of the grain because Zr is peritectic. However, the homogeneous distribution of the Al_3Zr particles improves and the fraction of Al_3Zr particles increases in two-stage homogenization scheme. At the first low-temperature (e.g., 400 °C) stage, the Al_3Zr particles are homogeneously precipitated at the center of the grain by homogeneous nucleation and may be heterogeneously nucleated on the residual second-phase particles at the grain boundary regions. At the second elevated-temperature (e.g., 470 °C) stage, the Al_3Zr nuclei become larger. A suitable two-stage homogenization scheme for the present 7085-type Al alloy is 400 °C/12 h + 470 °C/12 h.

Introduction

Homogenization is necessary for as-cast Al–Zn–Cu–Mg alloys, because the microsegregation of Zn, Cu, and Mg elements and coarse intermetallic particles results in poor properties [1–6]. In general, conventional homogenization aims to dissolve intermetallic particles into a matrix and reduce microsegregation. On the other hand, homogenization is widely known to cause precipitation of the Al_3Zr dispersoid in the wrought 7000 series Al alloys with the addition of zirconium [7, 8], because the metastable and coherent Al_3Zr dispersoid can reduce the fraction of recrystallization. The effectiveness of the Al_3Zr dispersoid in doing so depends on its size, spacing, and distribution [8–10]. Hence, special homogenization schemes have to be adopted [10, 11]. Several applications of the 7085 Al alloy, including in the Airbus A380, have been reported in literatures [12–14]. However, very few studies have focused on the as-cast and homogenized microstructures of this new-generation Al alloy, which is very important for attaining high strength, superior damage tolerance, and low quench sensitivity [15–17].

In present study, the microstructures of an Al–Zn–Mg–Cu alloy have been investigated before and after various homogenization schemes. The chemical composition of the present Al alloy is consistent with that of AA7085 registered with the Aluminum Association [15]. The purpose of the present study is to develop an initial understanding of the dissolution of the primary eutectic and the precipitation of Al_3Zr in the 7085-type Al alloy during homogenization. This will be useful for the optimization the microstructures and properties of the 7085 Al alloy during its manufacture.

Experiments

The materials under study were prepared through the ingot metallurgy route in the laboratory. The raw materials were high-purity Al (99.998%), Zn (99.98%), Mg (99.98%),

---

Y.-L. Deng · L. Wan (✉) · L.-H. Wu · Y.-Y. Zhang ·
X.-M. Zhang
School of Materials Science and Engineering,
Central South University, Changsha 410083, China
e-mail: wanli_csu@yeah.net

Y.-L. Deng · X.-M. Zhang
Key Laboratory of Nonferrous Materials Science and
Engineering, Ministry of Education, Changsha 410012, China

Table 1 Study of chemical composition of 7085 alloy investigated (wt%)

	Zn	Mg	Cu	Zr	Fe	Si	Cr	Mn	Ti	Al
AA7085	7.0–8.0	1.2–1.8	1.3–2.0	0.08–0.15	0.08	0.06	0.04	0.04	0.06	Bal.
Actual alloy	7.81	1.62	1.81	0.13	0.07	0.05	0.03	0.04	0.06	Bal.

Table 2 Homogenization heat treatments of samples

Sample number	Solution heat treatments
H400	400 °C/12 h
H450	450 °C/12 h
H470	470 °C/12 h
SH450	400 °C/12 h + 450 °C/12 h
SH470	400 °C/12 h + 470 °C/12 h

Al–3% Zr, Al–30% Cu, and Al–5% Ti–B (wt%). The alloy was melted in a graphite crucible heated by an electrical resistance furnace. The melting, refining, and casting temperatures were about 750–780 °C, 730–750 °C, and 710–720 °C, respectively. Liquid metal was then poured into an iron mold. The ingot dimensions were 30 × 80 × 120 mm. The chemical composition of the alloy was determined by wet chemical analysis as shown in Table 1. Slices with dimensions 10 × 13 × 13 mm were cut from the as-cast ingot. The differential scanning calorimetry (DSC) test indicated that the melting peak temperature of the primary eutectic in the as-cast ingot was about 475 °C. The slices were homogenized by various schemes, as shown in Table 2, with heat-up rates of 1.5 °C/min.

A combination of optical microscopy (OM), scanning electron microscopy (SEM), and energy dispersive X-ray spectrometry (EDS) was carried out to examine the microstructures in the as-cast and homogenized samples. SEM was carried out on a JSM-6360LV microscope with EDS. For the SEM examination, the samples were mechanically polished but unetched. The X-ray diffraction test was performed on a Rigaku D/Max 2500 automatic diffractometer. The precipitated Al_3Zr particles were characterized by transmission electron microscopy (TEM). Samples for TEM were thinned to about 80 μm followed by electropolishing in a twin-jet polishing unit operating at 15 V and −20 °C using a solution of 30% nitric acid and 70% methanol, and the disks were observed in a JEM 2100 microscope, operated at 200 kV.

Results and discussion

DSC and XRD results

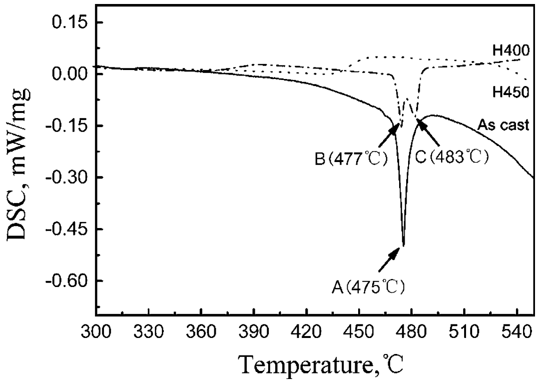

Fig. 1 DSC plots of as-cast and homogenized samples (H400: 400 °C/12 h, H470: 470 °C/12 h)

The DSC plots of the samples before and after homogenizations are shown in Fig. 1. One endothermic peak is identified at about 475 °C (denoted as A) on the DSC plot of the as-cast sample. Further observations show that the solidification eutectic in the non-equilibrium state should initially be melted at about 467 °C. However, there are two endothermic peaks on the DSC plot of the homogenized sample at 400 °C (denoted as H400). One of the peak points is 477 °C (denoted as B), and the other is 483 °C (denoted as C). This indicates that two kinds of second-phases have been melted until the temperature up to the melting point of the Al alloy matrix. The peak temperature of the point B should be the melting point of the residual eutectic particles, which is slightly higher than that of the as-cast sample. Such a shift is consistent with the slight increase in the melting temperature of the non-equilibrium solidification eutectic during homogenization. There will be further discussion on the peak temperature of the point C (483 °C) in the following sections. Furthermore, neither an endothermic nor an exothermic reaction is found in the homogenized sample at 470 °C (denoted as H470).

The XRD spectrums of the as-cast and homogenized samples are shown in Fig. 2. The patterns for the as-cast sample confirm that the primary eutectic mainly consisted of α (Al) and η-phases with the same crystallographic lattice constant as the $MgZn_2$ phase. Furthermore, the Al_2CuMg (S-phase) is only identified by the homogenized samples H400. Therefore, the peak point C at 483 °C on the DSC plot for the sample H400 (Fig. 1) should be the melting point of the S-phase. The details of the second phases by the results of DSC and XRD in various samples are shown in Table 3.

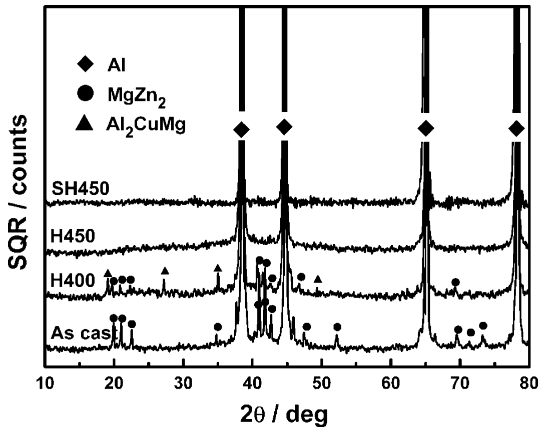

Fig. 2 X-ray diffraction patterns of as-cast and homogenized samples (H400: 400 °C/12 h, H450: 450 °C/12 h, and SH450: 400 °C/12 h + 450 °C/12 h)

Table 3 Statistics of phases detected by DSC and XRD in different samples

Sample number	Phase detected by X-ray diffraction		
	Al	$MgZn_2$	Al_2CuMg
As cast	√	√	×
H400	√	√	√
H450	√	×	×
SH450	√	×	×

Microstructures of the as-cast alloy

The SEM images of the as-cast sample are shown in Fig. 3a. The dark areas are the primary solid solution, and the bright areas are the non-equilibrium solidification eutectic between grains, which appear in a latticed pattern at higher magnification as showed in Fig. 3b. Since Zn/Mg is about 4.9 (>2.2) in the present alloy, the dominant second phase in the solidification eutectic should be the $MgZn_2$ phase, according to the phase diagram. Furthermore, some dispersal gray particles are also found, as indicated by the arrow in Fig. 3a. The stoichiometry of the dispersal gray particles is 67.66 at.% Al and 23.13 at.% Cu, as shown in Fig. 3c, which is close to the stoichiometry of Al_2Cu (θ-phase). The EDS results shown in Fig. 3d reveal that stoichiometry of the bright areas is 39.08 at.% Al, 18.98 at.% Zn, 26.98 at.% Mg, and 14.96 at.% Cu. Some Al and Cu atoms are assumed to have dissolved in the η-phase to form $Mg(Zn,Cu,Al)_2$, as indicated by previous investigations on the as-cast 7055 Al alloy [2, 5]. However, the stoichiometry of the gray particles is not consistent with that of $MgZn_2$ (η-phase). Hence, the second phase in the bright areas is probably $Mg(Zn,Cu,Al)_2$ with the same crystallographic lattice constant as $MgZn_2$. Of course, the Al_2CuMg phase would be embraced in the primary eutectic because it is composed of Al, Cu, and Mg elements too, but this is neither verified by the XRD results nor observed by the SEM. In short, since the as-cast ingot consists of a small amount of Al_2Cu and/or Al_2CuMg particles they cannot be determined by XRD and DSC tests, but Al_2Cu particles can be verified by SEM and EDS. The main second-phase in the as-cast ingot is the η-phase with stoichiometry of $Mg(Zn,Cu,Al)_2$, which is consistent with the above results of XRD, DSC, and SEM.

Evolution of coarse particle phases during homogenization

Typical SEM images of the microstructures after various homogenization schemes are shown in Fig. 4. A new phase close to the remained $Mg(Zn,Cu,Al)_2$ phase can be clearly observed in the sample H400, as shown in Fig. 4a. The EDS results of the newly formed phase are 57.40 at.% Al, 17.33 at.% Cu, 1.88 at.% Zn, and 23.39 at.% Mg, which is close to the stoichiometry of the S-phase. This has also been confirmed by the DSC plots (Fig. 1) and the XRD spectrums (Fig. 2). The SEM images of the homogenized microstructures in samples H450 and SH450 are shown in Fig. 4b, c, respectively. A small residual amount of second-phase particles is still found to be present in the samples. The EDS tests verify that these residual second-phase particles are S-phase, which is consistent with the results of the DSC that the melting point of S-phase is 483 °C.

The OM images of the microstructures after various homogenizations are shown in Fig. 5. A small amount of dark particles, which should be the Al_2CuMg phase, can be seen in the sample SH450 (Fig. 5a). However, the second-phase particles are almost invisible, and the grain boundaries are fine in the sample SH470 (Fig. 5b). These OM images again reveal that the primary Al_2Cu and $Mg(Zn,Cu,Al)_2$ particles have been dissolved into the matrix after homogenizations at 450 °C/12 h or 400 °C/12 h + 450 °C/12 h, but there is a significant presence of a few residual Al_2CuMg particles. It is no other than homogenization at 470 °C, the Al_2CuMg particles can be completely dissolved into the matrix quickly.

Precipitation behaviors of Al_3Zr particles

TEM images of Al_3Zr precipitation particles within the grains after various homogenizations are shown in Fig. 6. A large number of very fine (<10 nm) Al_3Zr dispersoid particles are precipitated in the sample H400, as shown in Fig. 6a, the distribution of Al_3Zr particles is homogenous. It is seen in the sample H470, as shown in Fig. 6b, that the number density of Al_3Zr dispersoid particles is much

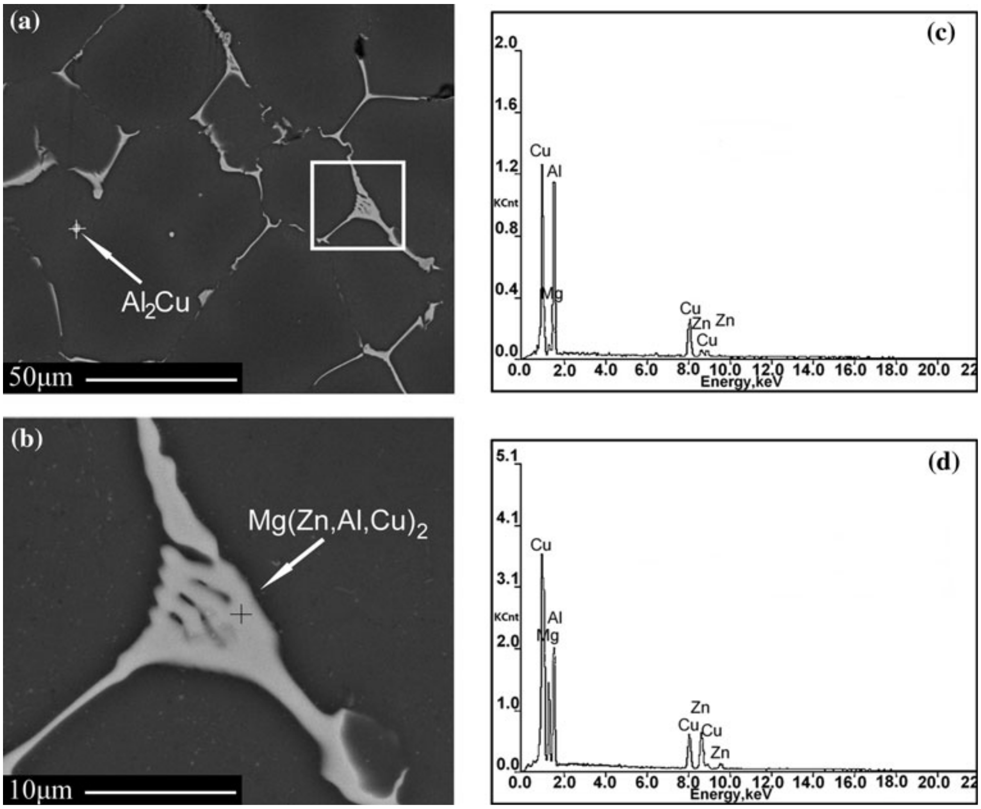

Fig. 3 Backscattered electron images of microstructures and EDS results in as-cast 7085-type Al alloy

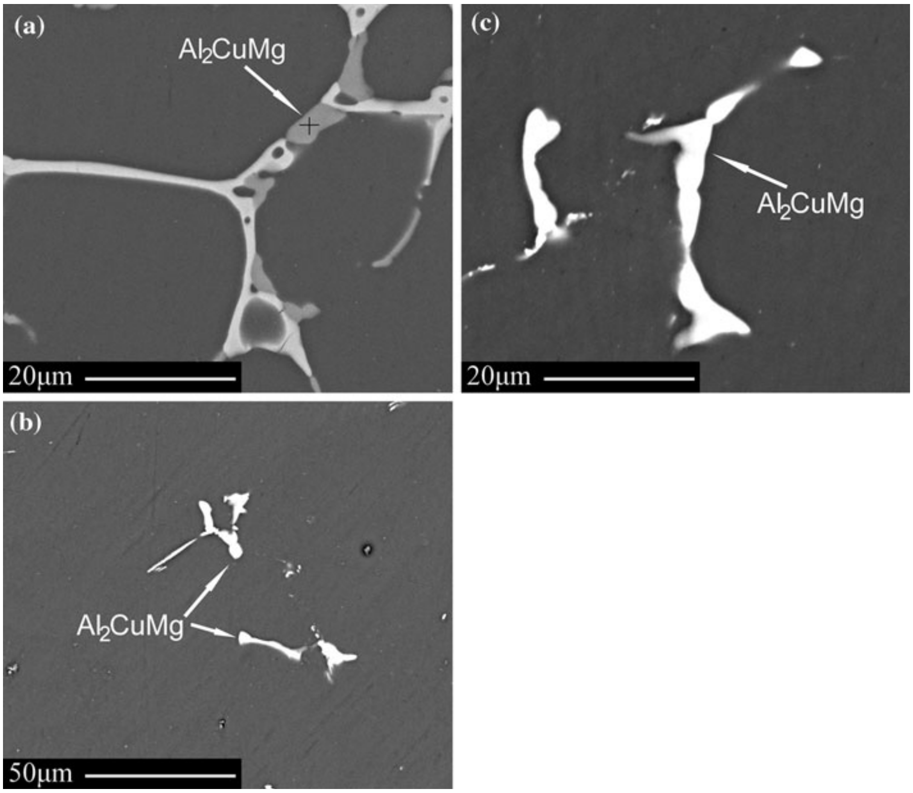

Fig. 4 Residual coarse phases after homogenizations at (**a**) H400: 400 °C/12 h, (**b**) H450: 450 °C/12 h, and (**c**) SH450: 400 °C/12 h + 450 °C/12 h

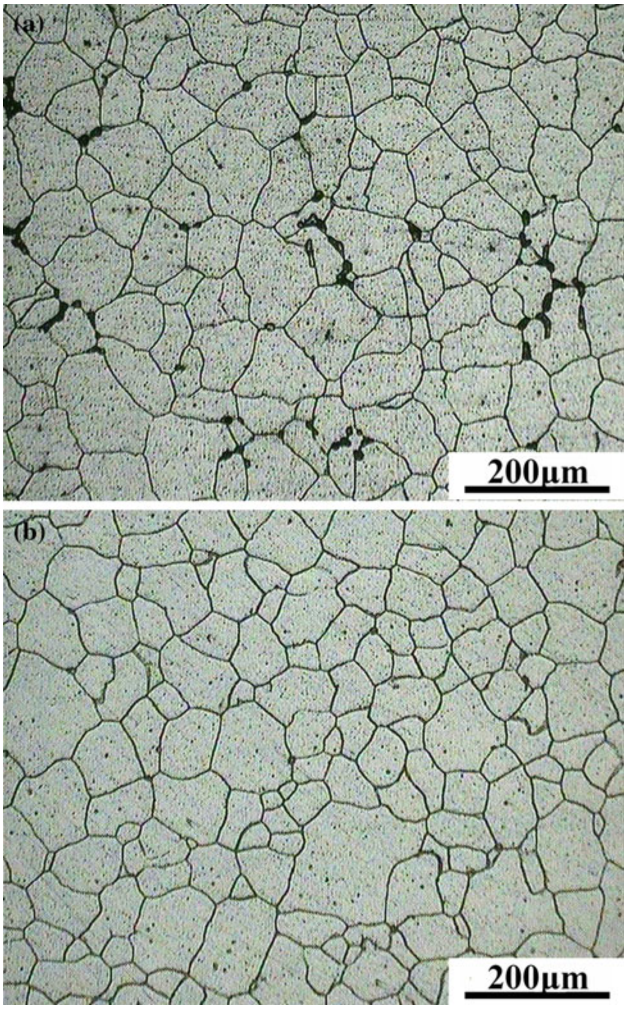

Fig. 5 Optical micrographs of the homogenized samples: (**a**) SH450: 400 °C/12 h + 450 °C/12 h and (**b**) SH470: 400 °C/12 h + 470 °C/12 h

smaller than that in the sample H400. Possibly, it is interpreted that the low temperature homogenization of the sample H400 leads to an increase in zirconium supersaturation, which provides the driving force for the precipitation of Al_3Zr. However, it is seen in the sample SH470, as shown in Fig. 6c, that the Al_3Zr dispersoid particles have a higher number density than that of H470, and have a greater size than H400. In other words, the fraction of Al_3Zr particles increases during the two-stage homogenization scheme as shown in Table 4.

The precipitation behavior of the Al_3Zr particles in the areas close to the grain boundaries is studied as shown in Fig. 7. The Al_3Zr precipitation particle is almost not found in the area close to the boundary in the sample H450 treated by a single-stage homogenization scheme (Fig. 7a). On the contrary, as shown in Fig. 7b, c, the number density of Al_3Zr particles is smaller, but their sizes are larger than those at the center of the grain in the sample treated by a two-stage homogenization scheme SH450. This shows that the two-stage homogenization scheme help promote the precipitation of the Al_3Zr particles in the area close to the grain boundaries as shown in Table 4.

The effect of homogenization schemes on precipitation behaviors of Al_3Zr particles may be interpreted as following. Zirconium element is subjected to segregation among the as-cast 7000 series Al alloys because it is peritectic, a high concentration of zirconium occurs at the center of the dendrites, while there is a low zirconium concentration near the grain boundaries. During single-stage homogenization schemes, the Al_3Zr particles are mainly precipitated at the center of the grain by homogeneous nucleation, and the number density of the precipitation of the Al_3Zr particles increases with decreasing temperature. Therefore, the number density of the Al_3Zr particles in the sample H400 is larger than that in the sample H470, but their size in the sample H400 is smaller (Fig. 6a, b). The low zirconium concentration probably results in little precipitation of Al_3Zr particles in the area near the grain boundaries (Fig. 7a). However, during two-stage homogenization schemes, at the first low-temperature (e.g., 400 °C) stage, the Al_3Zr particles are homogeneously precipitated at the center of the grain, which will serve as a nucleus for the subsequent growth; in the meantime, the Al_3Zr particles may be heterogeneously nucleated on those residual second-phase particles at the grain boundaries. At the second elevated-temperature (e.g., 470 °C) stage, the Al_3Zr nucleus becomes larger, and the residual second-phase particles are dissolved into the matrix. Therefore, the homogeneous distribution of the Al_3Zr particles improves, and the fraction of Al_3Zr particles increases (Figs. 6c and 7b, c) at either the center or the boundary regions within a grain scale. In the present study, a suitable two-stage homogenization scheme is 400 °C/12 h + 470 °C/12 h.

Conclusions

(1) The as-cast 7085-type Al alloy mainly contains the α-phase (Al), non-equilibrium solidification eutectic, and dispersal Al_2Cu phase. Some eutectic gets transformed into the Al_2CuMg phase at 400 °C. The primary eutectic and dispersal Al_2Cu particles gradually dissolve into the matrix at 450 °C.

(2) The precipitation behaviors of Al_3Zr particles are affected by homogenization schemes. The Al_3Zr particles are mainly precipitated at the center of the grain because Zr is peritectic during single-stage homogenization.

(3) The homogeneous distribution of the Al_3Zr particles improves, and the fraction of Al_3Zr particles

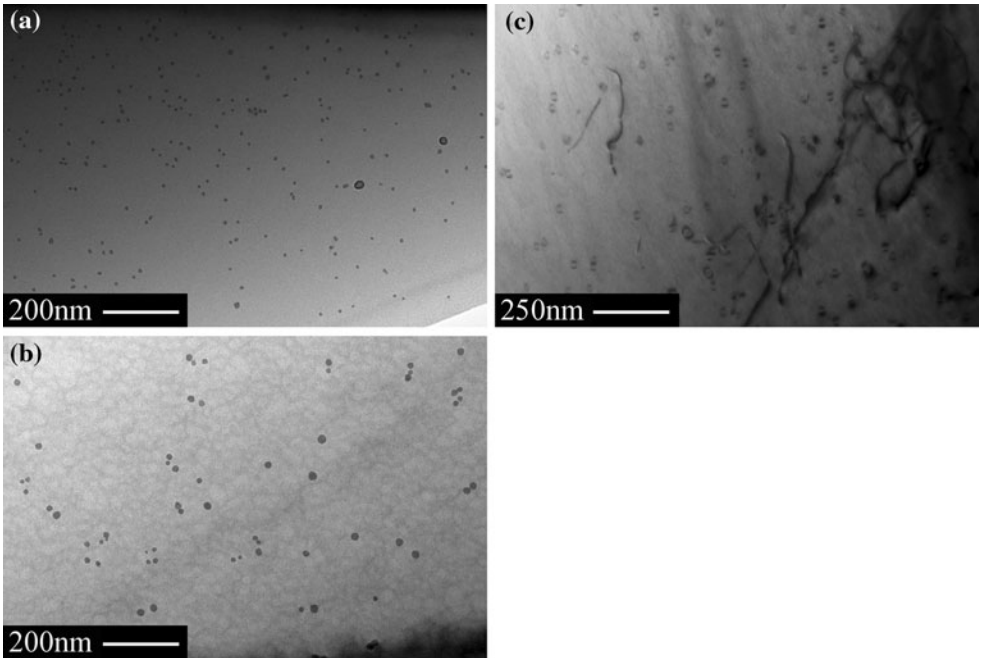

Fig. 6 Precipitations of AI_3Zr particles within a grain after homogenizations at (**a**) H400: 400 °C/12 h, (**b**) H470: 470 °C/12 h, and (**c**) SH470: 400 °C/12 h + 470 °C/12 h

Table 4 Statistical measure of number density of Al_3Zr particles in different regions (μm^{-2})

Sample number	Near grain boundaries	In the middle of grains
H450	3 ± 1	77 ± 2
SH450	13 ± 2	95 ± 2
H470	2 ± 1	72 ± 2
SH470	14 ± 2	94 ± 2

increases during the two-stage homogenization scheme. At the first low-temperature (400 °C) stage, the Al_3Zr particles are homogeneously precipitated at the center of the grain by homogeneous nucleation, and may be heterogeneously nucleated on the residual second-phase particles at the grain boundary regions. At the second elevated-temperature (470 °C) stage, the Al_3Zr nuclei become larger.

Fig. 7 Precipitations of AI_3Zr particles in region close to grain boundary after homogenizations at (**a**) H450: 450 °C/12 h and (**b**, **c**) SH450: 400 °C/12 h + 450 °C/12 h

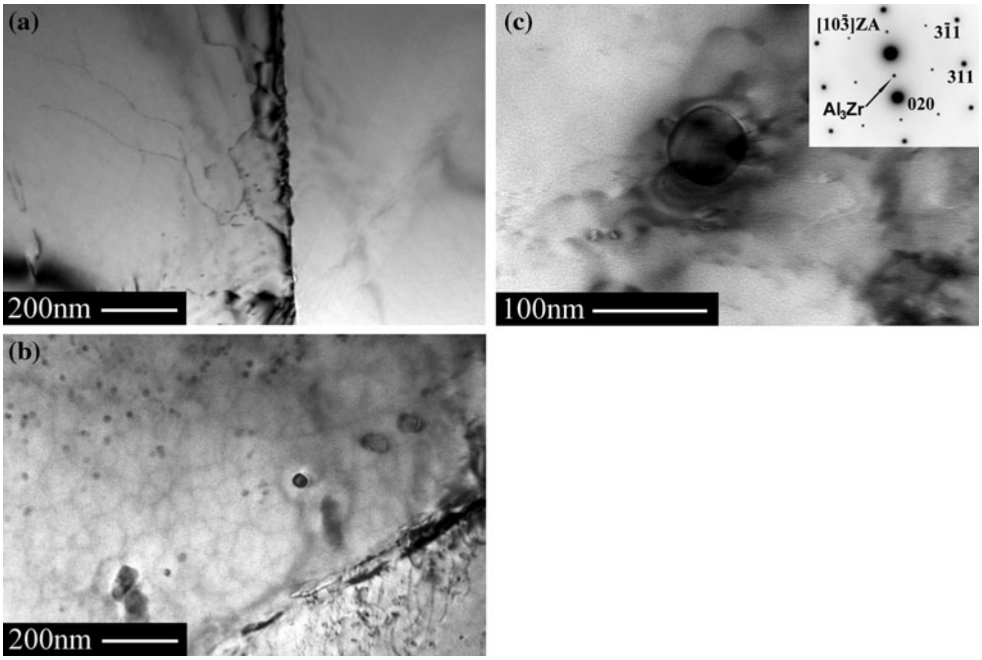

(4) A suitable two-stage homogenization scheme for the present 7085-type Al alloy is 400 °C/12 h + 470 °C/12 h.

Acknowledgements The authors gratefully acknowledge the financial support by the National Basic Program of China (No. 2005CB623700).

References

1. Li YX, Li P, Zhao G, Liu XT, Cui JZ (2005) Mater Sci Eng A 397:204
2. Mondal C, Mukhopadhyay AK (2005) Mater Sci Eng A 391:367
3. Xie FY, Yan XY, Ding L, Zhang F, Chen SG, Chu MG, Chang YA (2003) Mater Sci Eng A 355:144
4. Li H, Cao DH, Wang ZX, Zheng ZQ (2008) J Mater Sci 43:1583. doi:10.1007/s10853-007-2346-7
5. Fan XG, Jiang DM, Meng QC, Zhong L (2006) Mater Lett 60:1475
6. Toda H, Kobayashi T, Takahashi A (2000) Mater Sci Eng A 280:69
7. Zedalis MS, Fine ME (1986) Metall Trans A 17:2187
8. Robson JD (2002) Mater Sci Eng A 338:219
9. Robson JD, Prangnell PB (2001) Acta Mater 49:599
10. Morere B, Maurice C, Shahani R, Driver J (2001) Metall Mater Trans A 32A:625
11. Chakrabarti DJ, Liu J, Goodman JH, Venema GB, Sawtell RR, Krist CM, Westerlund RW (2005) US Patent 6-972-110 B2, December 6
12. Karabin ME, Barlat F, Schultz RW (2007) J Mater Process Technol 189:45–57
13. Luong H, Hill MR (2008) Mater Sci Eng A 477:208
14. Shuey RT, Barlat F, Karabin ME, Chakrabarti DJ (2009) Metall Mater Trans A 40:365
15. Boselli J, Chakrabarti DJ, Shuey RT (2008) In: Proc ICAA11. Wiley-VCH, Weinheim, pp 202–208
16. Chakrabarti DJ, Liu J, Sawtell RR, Venema GB (2004) Mater Forum 28:969
17. Liu J (2006) Mater Sci Forum 519–512:1233